pp 1811–1825. © Royal Aeronautical Society 2018
doi:10.1017/aer.2018.94

Novel guidance model and its application for optimal re-entry guidance

C.W. Jiang and G.F. Zhou
cwjiang2010@163.com
China Academy of Launch Vehicle Technology
Beijing
China

B. Yang, C.S. Gao and W.X. Jing
School of Astronautics
Harbin Institute of Technology
Harbin
China

ABSTRACT

Aiming at three-dimensional (3D) terminal guidance problem, a novel guidance model is established in this paper, in which line-of-sight (LOS) range is treated as an independent variable, describing the relative motion between the vehicle and the target. The guidance model includes two differential equations that describe LOS's pitch and yaw motions in which the pitch motion is separately decoupled. This model avoids the inaccuracy of simplified two-dimensional (2D) guidance model and the complexity of 3D coupled guidance model, which not only maintains the accuracy but also simplifies the guidance law design. The application of this guidance model is studied for optimal re-entry guidance law with impact angle constraint, which is presented in the form of normal overload. Compared with optimal guidance laws based on traditional guidance model, the proposed one based on novel guidance model is implemented with the LOS range instead of time-to-go, which avoids the problem of the time-to-go estimation of traditional optimal guidance laws. Finally, the correctness and validity of the guidance model and guidance law are verified by numerical simulation. The guidance model and guidance law proposed in this paper provide a new way for the design of terminal guidance.

Keywords: Terminal guidance; Guidance model; LOS range; Optimal guidance law; Impact angle constraint

Received 2 January 2018; revised 29 April 2018; accepted 29 June 2018

NOMENCLATURE

V_M	velocity vector of the vehicle
r	LOS range
θ	azimuth angle of LOS
φ	elevation angle of LOS
θ_M	heading angle
φ_M	flight path angle

1.0 INTRODUCTION

Terminal guidance law guides the vehicle towards the target according to their relative motion with high precision, during which certain path constraints and terminal constraints have to be satisfied. The design of terminal guidance includes two parts: the guidance model description (e.g. the relative motion of the vehicle and the target) and the guidance algorithm design, in which the description of 3-dimensional (3D) guidance model with low complexity and high accuracy plays a key role in terminal guidance design. On the one hand, the guidance model is the foundation of the guidance algorithm design, the complexity of which directly determines the difficulty of the guidance algorithm design. On the other hand, the guidance model is the mathematical expression of actual relative motion of the vehicle and the target, the accuracy of which directly determines whether the theoretical precision of resulting guidance law can be achieved in engineering.

Existing 3D guidance model can be mainly classified into three categories. The first category is that under conditions of small LOS angle and angular rate, the relative motion equation with respect to time is linearized about the collision course, and then 3D guidance model can be simplified into two 2-dimensional (2D) guidance models. According to this idea, 2D guidance models of the pitch and yaw plane of LOS are established separately in Refs 1,2 and then optimal guidance law with terminal angle constraint is designed. In Refs 3,4, simplified guidance model of the pitch plane of LOS is established, and then sliding mode guidance law with disturbance suppression is designed to make LOS angular rate converges to zero with stability. Based on simplified guidance model of the pitch plane of LOS, H_∞/H_2 robust guidance law and Lyapunov-based non-linear guidance law are proposed, respectively, in Refs. 5,6. Based on simplified 2D guidance model, finite-time convergent guidance law accounting for autopilot lag are studied in Refs 7–9, theoretically proving that LOS angular rate converges to zero in finite time. The first category of guidance model ignores the coupling between the pitch motion and the yaw motion of LOS, which simplifies the guidance law design, but not strict in theory. When LOS angle and angular rate are large, the coupling among actual 3D guidance model is serious and the accuracy of simplified 2D guidance model is poor, for which it is difficult to guarantee the theoretical precision of resulting guidance law in engineering.

The second category is that the 3D guidance model is established in the body coordinate system with respect to time, in which different channels are coupled with each other. Based on 3D-coupled guidance model in the body co-ordinate system, performance of pure proportional navigation guidance law is analysed in Refs 10,11. The third category is that the 3D guidance model is established in LOS coordinate system with respect to time, in which the pitch motion and the yaw motion of LOS are coupled with each other. Based on 3D coupled guidance model in LOS coordinate system, analytical solution and capturability of true

proportional navigation guidance law are discussed in Refs 12,13. The second and third categories of guidance model describe the relative motion of the vehicle and the target accurately, but the models are relatively complex and the coupling among different channels is serious, for which the performance of resulting proportional navigation guidance laws is poor when the target escapes with high maneuvering acceleration. In Refs 14–16, 3D coupled guidance model is linearized using feedback linearization approach, and then robust guidance laws are designed. To suppress the coupling term of 3D coupled guidance model, non-linear robust guidance laws are designed in Refs 17–19. Although robust guidance laws can suppress the non-linear coupling term and external disturbance of the guidance model, rapidity of the system is reduced while robustness of the system is improved, for which the resulting guidance laws are too conservative. In Refs 20–22, extended state observer is introduced to estimate the coupling term and external disturbance of 3D-coupled guidance model, and then guidance laws are designed to suppress the coupling term and external disturbance of the guidance model. But the resulting guidance laws are complex, which is difficult to be achieved in engineering.

All in all, the first category of guidance model with respect to time ignores the coupling among different channels so that the design of guidance law is simplified, but the guidance model is not accurate enough and it is difficult to guarantee the theoretical precision of resulting guidance laws in engineering. The second and third categories of guidance model with respect to time take a full consideration of the coupling among different channels so that the accuracy of the model is guaranteed, but the coupling term of the guidance model is not convenient for the design of guidance law. In this paper, aiming at describing the relative motion of the vehicle and the target simply and accurately, a novel guidance model is established in which LOS range is treated as independent variable. The guidance model includes two differential equations that describe LOS's pitch and yaw motions in which the pitch motion is separately decoupled. The guidance model not only maintains the accuracy but also simplifies the guidance law design. Then, the application of this guidance model is studied for optimal re-entry guidance law with impact angle constraint, which is presented in the form of normal overload. Finally, numerical simulation verifies the correctness and validity of the guidance model and guidance law.

2.0 NOVEL GUIDANCE MODEL WITH RESPECT TO LOS RANGE

The vehicle-target engagement geometry in 3D space is shown in Fig. 1, in which M denotes the mass centre of the vehicle; T denotes the target. $L(O_L - X_L Y_L Z_L)$ is the re-entry co-ordinate system, where the origin O_L is located at the intersection of the earth's surface and the right line between the earth centre and the vehicle mass centre at the initial moment of re-entry; $O_L X_L$ points to the east in the local horizontal plane; $O_L Z_L$ is located perpendicularly to the local horizontal plane and points to the above; $O_L Y_L$ along with $O_L X_L$ and $O_L Z_L$ constitute the right-hand Cartesian coordinate system. $S(M - e_r e_\theta e_\phi)$ is the LOS co-ordinate system, where the origin is located at the vehicle mass centre; Me_r points to the target along the LOS; Me_ϕ is located perpendicularlyly to Me_r in the vertical plane of LOS and points to the above; Me_θ along with Me_r and Me_ϕ constitute the right-hand Cartesian coordinate system. $A(M - X_A Y_A Z_A)$ is the velocity azimuth coordinate system, where the origin is located at the vehicle mass centre; MX_A coincides with $\mathbf{V_M}$; MZ_A is located perpendicularly to MX_A in the vertical

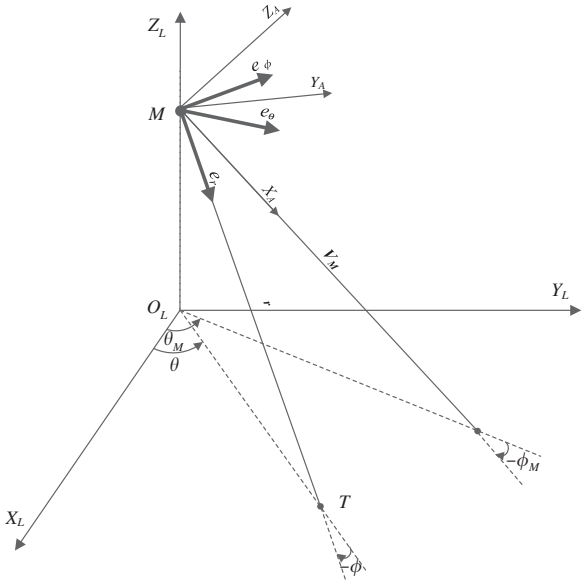

Figure 1. 3D vehicle-target engagement geometry.

plane of $\mathbf{V_M}$ and points to the above; MY_A along with MX_A and MZ_A constitute the right-hand Cartesian co-ordinate system.

What is more, the re-entry co-ordinate system can be transformed to the LOS coordinate system by rotating θ and $-\phi$ anti-clockwise around O_LZ_L and O_LY_L in turn. The re-entry coordinate system can be transformed to the velocity azimuth co-ordinate system by rotating θ_M and $-\phi_M$ anti-clockwise around O_LZ_L and O_LY_L in turn. Δ_ϕ is the included angle between the velocity vector $\mathbf{V_M}$ and the vertical plane of O_Me_r; Δ_θ is the included angle between O_Me_r and the component of $\mathbf{V_M}$ in the vertical plane of O_Me_r. The LOS coordinate system can be transformed to the velocity azimuth coordinate system by rotating Δ_θ, $-\Delta_\phi$ and Δ_γ anti-clockwise around O_Me_θ, O_Me_ϕ and O_Me_r in turn.

Assume that the vehicle attacks a fix target on the ground, then under the definitions above, kinematical equations of the relative motion between the vehicle and the target can be described as

$$\begin{cases} \dot{r} = -V_M\cos\Delta_\phi\cos\Delta_\theta \\ \dot{\phi} = \frac{1}{r}V_M\cos\Delta_\phi\sin\Delta_\theta \\ \dot{\theta}\cos\phi = \frac{1}{r}V_M\sin\Delta_\phi \end{cases} \quad \cdots(1)$$

Define $\dot{\overline{\theta}}$, B_r, B_ϕ, B_θ and $\overline{V}_M$ as follows:

$$\begin{cases} \dot{\overline{\theta}} = \dot{\theta}\cos\phi \\ B_r = \cos\Delta_\theta \\ B_\phi = \sin\Delta_\theta \\ B_\theta = \sin\Delta_\phi \\ \overline{V}_M = V_M\cos\Delta_\phi \end{cases} \quad \cdots(2)$$

then, (1) can be rewritten as follows:

$$\begin{cases} \dot{r} = -\overline{V}_M B_r \\ \dot{\phi} = \frac{1}{r}\overline{V}_M B_\phi \\ \dot{\overline{\theta}} = \frac{1}{r} V_M B_\theta \end{cases} \quad \cdots(3)$$

According to the rules of differentiation, we can get

$$\begin{cases} \dot{\phi} = \frac{d\phi}{dt} = -\dot{r}\frac{d\phi}{d(-r)} \\ \dot{\theta} = \frac{d\theta}{dt} = -\dot{r}\frac{d\theta}{d(-r)} \end{cases} \quad \cdots(4)$$

First and second derivatives of variable Δ with respect to $-r$ are, respectively, denoted as Δ' and Δ''. Now that $\dot{r}$ is usually non-zero in the guidance process, then (4) can be rewritten as follows:

$$\begin{cases} \phi' = -\frac{1}{\dot{r}}\dot{\phi} \\ \theta' = -\frac{1}{\dot{r}}\dot{\theta} \end{cases} \quad \cdots(5)$$

Substituting (5) into (3), we have

$$\begin{cases} \dot{r} = -\overline{V}_M B_r \\ \phi' = -\frac{1}{r\dot{r}}\overline{V}_M B_\phi \\ \overline{\theta}' = -\frac{1}{r\dot{r}} V_M B_\theta \end{cases} \quad \cdots(6)$$

where $\overline{\theta}' = \theta' \cos\phi$.

Assume that V_M is constant, then differentiating (6) with respect to $-r$, we get

$$\begin{cases} \phi'' - \frac{1}{r}\phi' = \frac{\overline{V}_M^2}{r\dot{r}^2}(B_\phi' B_r - B_\phi B_r') \\ \overline{\theta}'' - \frac{1}{r}\overline{\theta}' = \frac{V_M \overline{V}_M}{r\dot{r}^2}(B_\theta' B_r - B_\theta B_r') - \frac{V_M B_\theta B_r \overline{V}_M'}{r\dot{r}^2} \end{cases} \quad \cdots(7)$$

From (2), we can obtain

$$\begin{cases} B_r' = -\Delta_\theta' \sin\Delta_\theta \\ B_\phi' = \Delta_\theta' \cos\Delta_\theta \\ B_\theta' = \Delta_\phi' \cos\Delta_\phi \\ \overline{V}_M' = -V_M \Delta_\phi' \sin\Delta_\phi \end{cases} \quad \cdots(8)$$

Substituting (2) and (8) into (7), we have

$$\begin{cases} \phi'' - \frac{1}{r}\phi' = \frac{\overline{V}_M^2}{r\dot{r}^2}\Delta_\theta' = \frac{\Delta_\theta'}{r\cos^2\Delta_\theta} \\ \overline{\theta}'' - \frac{1}{r}\overline{\theta}' = \frac{\Delta_\phi'}{r\cos^2\Delta_\phi\cos\Delta_\theta} + \frac{\Delta_\theta'\sin\Delta_\theta\sin\Delta_\phi}{r\cos\Delta_\phi\cos^2\Delta_\theta} \end{cases} \quad \cdots(9)$$

(9) is the resulting novel guidance model with respect to $-r$.

Remark 1. The guidance model includes two differential equations that describe LOS's pitch and yaw motions in which the pitch motion is separately decoupled. Compared with the first[1,2] category of guidance model, this guidance model increases the accuracy while maintaining low complexity, which is more congruent with actual guidance process. Compared with the second[10,11] and third[12,13] categories of guidance model, this guidance model reduces the complexity while maintaining the accuracy, which is more convenient for the guidance law design.

3.0 APPLICATION OF THE NOVEL GUIDANCE MODEL

3.1 Optimal re-entry guidance law with impact angle constraint

(1) Guidance law in the pitch plane of LOS

From (9), we can obtain the differential equation of the pitch motion of LOS

$$\phi''-\frac{1}{r}\phi'=\frac{\overline{V}_M^2}{r\dot{r}^2}\Delta_\theta'=\frac{\Delta_\theta'}{r\cos^2\Delta_\theta} \quad \cdots(10)$$

To guarantee the attack precision, design objective of the guidance law is selected to be zero LOS angular rate[23]. Meanwhile, impact angle constraint has to be satisfied to improve the attack performance. Thus, terminal constraints of the pitch motion are set as

$$\begin{cases}\phi'(-r_f)=0\\ \phi(-r_f)=\phi_f\end{cases} \quad \cdots(11)$$

where ϕ_f is the desired impact angle.

For the convenience of description, the variables $\phi-\phi_f$, ϕ' and ϕ'' are respectively denoted as x, x' and x'', then (10) and (11) can be written as follows:

$$\begin{cases}x''-\frac{1}{r}x'=\frac{u}{r}\\ x(-r_f)=0\\ x'(-r_f)=0\end{cases} \quad \cdots(12)$$

where $u=\Delta_\theta'/\cos^2\Delta_\theta$.

Rewriting (12) in state-space form, we have

$$\begin{cases}X'=A(-r)X+B(-r)u\\ X(-r_f)=\begin{bmatrix}0\\0\end{bmatrix}\end{cases} \quad \cdots(13)$$

where $X=\begin{bmatrix}x_1\\x_2\end{bmatrix}=\begin{bmatrix}x\\x'\end{bmatrix}$, $A(-r)=\begin{bmatrix}0&1\\0&\frac{1}{r}\end{bmatrix}$, $B(-r)=\begin{bmatrix}0\\\frac{1}{r}\end{bmatrix}$.

To satisfy the terminal constraints and achieve the maximum terminal velocity, cost functional can be selected as follows:

$$J=X^TSX\big|_{-r=-r_f}+\int_{-r_0}^{-r_f}\left(u^TV(-r)u\right)d(-r) \quad \cdots(14)$$

where $S=\begin{bmatrix}\infty&0\\0&\infty\end{bmatrix}$, $V(-r)=[1]$.

Then, the guidance law design problem is transformed to the typical linear quadratic optimal control problem with the optimal solution in the interval $[-r_0,\ -r_f]$

$$u^*(-r)=-V^{-1}(-r)B^T(-r)P(-r)X(-r) \quad \cdots(15)$$

where $P(-r)$ is the symmetric matrix satisfying the following inverse Riccati equation:

$$\begin{cases}P'^{-1}(-r)=A(-r)P^{-1}(-r)+P^{-1}(-r)A^T(-r)-B(-r)V^{-1}(-r)B^T(-r)\\ P^{-1}(-r_f)=S^{-1}\end{cases} \quad \cdots(16)$$

Denote $Q(-r)$ as follows:

$$Q(-r)=P^{-1}(-r)=\begin{bmatrix} q_1 & q_3 \\ q_3 & q_2 \end{bmatrix}$$

then substituting $Q(-r)$ into (16), we have

$$\begin{cases} q'_1=2q_3 \\ q'_2=\frac{2q_2}{r}-\frac{1}{r^2} \\ q'_3=\frac{q_3}{r}+q_2 \end{cases} \quad \cdots(17)$$

where $q_1(-r_f)=0$, $q_2(-r_f)=0$ and $q_3(-r_f)=0$.

Analytical solution of (17) can be get that

$$\begin{cases} q_1=2c_3\ln r+c_2\ln^2 r+2r+c_1 \\ q_2=\frac{c_2}{r^2}+\frac{1}{r} \\ q_3=-\frac{c_3}{r}-\frac{c_2}{r}\ln r-1 \end{cases} \quad \cdots(18)$$

Now that $q_1(-r_f)=0$, $q_2(-r_f)=0$ and $q_3(-r_f)=0$, we have

$$\begin{cases} c_1=-r_f\left[1+(1-\ln r_f)^2\right] \\ c_2=-r_f \\ c_3=-r_f(1-\ln r_f) \end{cases} \quad \cdots(19)$$

According to (18) and (19), we can obtain that

$$\begin{cases} q_1=-2(-r+r_f)-r_f\left\{[\ln r-\ln r_f]^2+2[\ln r-\ln r_f]\right\} \\ q_2=-\frac{-r+r_f}{r^2} \\ q_3=\frac{(-r+r_f)+r_f[\ln r-\ln r_f]}{r} \end{cases} \quad \cdots(20)$$

By matrix inversion operation, we get

$$P(-r)=\begin{bmatrix} p_1 & p_3 \\ p_3 & p_2 \end{bmatrix} \quad \cdots(21)$$

where

$$\begin{cases} p_1=\frac{-(-r+r_f)}{(-r+r_f)^2-r\cdot r_f[\ln r-\ln r_f]^2} \\ p_2=\frac{-2(-r+r_f)-r_f\left\{[\ln r-\ln r_f]^2+2[\ln r-\ln r_f]\right\}}{(-r+r_f)^2-r\cdot r_f[\ln r-\ln r_f]^2}\cdot r^2 \\ p_3=-\frac{-r+r_f+r_f[\ln r-\ln r_f]}{(-r+r_f)^2-r\cdot r_f[\ln r-\ln r_f]^2}\cdot r \end{cases}$$

By substituting *R(–r)*, *B(–r)* and *P(–r)* into (15), optimal solution of (13) can be get that

$$u^*(-r)=p_3\cdot\frac{x_1}{-r}+p_2\cdot\frac{x_2}{-r} \quad \cdots(22)$$

Then the guidance law of the pitch motion with respect to $-\boldsymbol{r}$ is described as

$$\Delta'_\theta=(\cos^2\Delta_\theta)\left(p_3\cdot\frac{\phi-\phi_f}{-r}+p_2\cdot\frac{\phi'}{-r}\right) \quad \cdots(23)$$

Furthermore, the guidance law of the pitch motion with respect to time is described as

$$\dot{\Delta}_\theta = (\cos^2\Delta_\theta)\left(p_3 \cdot \frac{\phi-\phi_f}{-r}(-\dot{r}) + p_2 \cdot \frac{\dot{\phi}}{-r}\right) \quad \cdots(24)$$

(2) Guidance law in the yaw plane of LOS

From (9), we can obtain the differential equation of the yaw motion of LOS

$$\overline{\theta}'' - \frac{1}{r}\overline{\theta}' = \frac{\Delta'_\phi}{r\cos^2\Delta_\phi\cos\Delta_\theta} + \frac{\Delta'_\theta\sin\Delta_\theta\sin\Delta_\phi}{r\cos\Delta_\phi\cos^2\Delta_\theta} \quad \cdots(25)$$

Similarly, angular rate of LOS in the yaw plane should be confined to zero to guarantee the attack precision[23], that is $\theta'(-r_f)=0$. Now that $\overline{\theta}' = \theta'\cos\phi$, when $\cos\phi(-r_f)$is not zero, terminal constraint of the yaw motion can be set as

$$\overline{\theta}'(-r_f) = 0 \quad \cdots(26)$$

The variables $\overline{\theta}'$ and $\overline{\theta}''$ are, respectively, denoted as x and x', then (25) and (26) can be written as follows:

$$\begin{cases} x' = \frac{1}{r}x + \frac{1}{r}u \\ x(-r_f) = 0 \end{cases} \quad \cdots(27)$$

where $u = \frac{\Delta'_\phi}{\cos^2\Delta_\phi\cos\Delta_\theta} + \frac{\Delta'_\theta\sin\Delta_\theta\sin\Delta_\phi}{\cos\Delta_\phi\cos^2\Delta_\theta}$.

Rewriting (27) in state-space form, we have

$$\begin{cases} x' = a(-r)x + b(-r)u \\ x(-r_f) = 0 \end{cases} \quad \cdots(28)$$

where $a(-r) = \frac{1}{r}, b(-r) = \frac{1}{r}$.

To satisfy the terminal constraints and achieve the maximum terminal velocity, cost functional can be selected as follows:

$$J = x^T sx\big|_{-r=-r_f} + \int_{-r_0}^{-r_f}(u^T v(-r)u)\mathrm{d}(-r) \quad \cdots(29)$$

where $s=\infty$, $v(-r)=1$.

Then, the guidance law design problem is transformed to the typical linear quadratic optimal control problem with the optimal solution in the interval $[-r_0, -r_f]$

$$u^*(-r) = -v^{-1}(-r)b^T(-r)p(-r)x(-r) \quad \cdots(30)$$

where $p(-r)$ satisfies the following inverse Riccati equation:

$$\begin{cases} p'^{-1}(-r) = \frac{2}{r}p^{-1}(-r) - \frac{1}{r^2} \\ p^{-1}(-r_f) = 0 \end{cases} \quad \cdots(31)$$

Analytical solution of (31) is of the following form:

$$p(-r) = -\frac{r^2}{-r+r_f} \quad \cdots(32)$$

By substituting $v(-r)$, $b(-r)$ and $p(-r)$ into (30), optimal solution of (28) can be get that

$$u^*(-r) = \frac{r}{-r+r_f} \cdot x \qquad \cdots(33)$$

then the guidance law of the yaw motion with respect to $-r$ is given as follows:

$$\Delta'_\phi = \cos^2\Delta_\phi \cos\Delta_\theta \left[-\frac{-r}{-r+r_f} \cdot \theta' \cos\phi - \frac{\Delta'_\theta \sin\Delta_\theta \sin\Delta_\phi}{\cos\Delta_\phi \cos^2\Delta_\theta} \right] \qquad \cdots(34)$$

Furthermore, the guidance law of the yaw motion with respect to time is described as

$$\dot{\Delta}_\phi = \cos^2\Delta_\phi \cos\Delta_\theta \left[-\frac{-r}{-r+r_f} \cdot \dot{\theta} \cos\phi - \frac{\dot{\Delta}_\theta \sin\Delta_\theta \sin\Delta_\phi}{\cos\Delta_\phi \cos^2\Delta_\theta} \right] \qquad \cdots(35)$$

Remark 2. Traditional guidance model is established with respect to time, and the optimal guidance law based on traditional guidance model is implemented with the time-to-go which is unknown and should be estimated[1,2]. Proposed guidance model in this paper is established with respect to LOS range, and the optimal guidance law based on proposed guidance model is implemented with the LOS range which can be obtained directly, and hence avoids the problem of the time-to-go estimation of traditional optimal guidance laws.

3.2 Guidance law in overload form

According to the definitions of coordinate systems in Section 2, there are two manners for transforming the re-entry coordinate system to the velocity azimuth coordinate system.

The first transformation manner is that by rotating θ and $-\phi$ anti-clockwise around $O_L Z_L$ and $O_L Y_L$ in turn, the re-entry coordinate system can be transformed to the LOS coordinate system. Further, by rotating Δ_θ, $-\Delta_\phi$ and Δ_γ anti-clockwise around Me_θ, Me_ϕ and Me_r in turn, the LOS coordinate system can be transformed to the velocity azimuth coordinate system. The rotational angular velocity of the velocity azimuth co-ordinate system with respect to re-entry coordinate system can be described as

$$\overline{\Omega} = \dot{\Delta}_\gamma - \dot{\Delta}_\phi + \dot{\Delta}_\theta - \dot{\phi} + \dot{\theta} \qquad \cdots(36)$$

Define $L_x(\eta)$, $L_y(\eta)$ and $L_z(\eta)$ as

$$L_x(\eta) = \begin{bmatrix} 1 & 0 & 0 \\ 0 & \cos\eta & \sin\eta \\ 0 & -\sin\eta & \cos\eta \end{bmatrix}, \quad L_y(\eta) = \begin{bmatrix} \cos\eta & 0 & -\sin\eta \\ 0 & 1 & 0 \\ \sin\eta & 0 & \cos\eta \end{bmatrix},$$
$$L_z(\eta) = \begin{bmatrix} \cos\eta & \sin\eta & 0 \\ -\sin\eta & \cos\eta & 0 \\ 0 & 0 & 1 \end{bmatrix} \qquad \cdots(37)$$

Then, components of the vector $\overline{\Omega}$ with respect to velocity azimuth coordinate system can be derived as

$$\begin{aligned}\begin{bmatrix}\overline{\Omega}_{x_A}\\ \overline{\Omega}_{y_A}\\ \overline{\Omega}_{z_A}\end{bmatrix} &= \begin{bmatrix}\dot{\Delta}_\gamma\\ 0\\ 0\end{bmatrix} + L_x(\Delta_\gamma)\begin{bmatrix}0\\ 0\\ -\dot{\Delta}_\phi\end{bmatrix} + L_x(\Delta_\gamma)L_z(-\Delta_\phi)\begin{bmatrix}0\\ \dot{\Delta}_\theta-\dot{\phi}\\ 0\end{bmatrix}\\ &\quad + L_x(\Delta_\gamma)L_z(-\Delta_\phi)L_y(\Delta_\theta-\phi)\begin{bmatrix}0\\ 0\\ \dot{\theta}\end{bmatrix}\\ &= \begin{bmatrix}-\dot{\theta}\cos\Delta_\phi\sin(\Delta_\theta-\phi)-(\dot{\Delta}_\theta-\dot{\phi})\sin\Delta_\phi+\dot{\Delta}_\gamma\\ \cos\Delta_\gamma\left[-\dot{\theta}\sin\Delta_\phi\sin(\Delta_\theta-\phi)+(\dot{\Delta}_\theta-\dot{\phi})\cos\Delta_\phi\right]+\sin\Delta_\gamma\left[\dot{\theta}\cos(\Delta_\theta-\phi)-\dot{\Delta}_\phi\right]\\ -\sin\Delta_\gamma\left[-\dot{\theta}\sin\Delta_\phi\sin(\Delta_\theta-\phi)+(\dot{\Delta}_\theta-\dot{\phi})\cos\Delta_\phi\right]+\cos\Delta_\gamma\left[\dot{\theta}\cos(\Delta_\theta-\phi)-\dot{\Delta}_\phi\right]\end{bmatrix}\end{aligned} \quad \cdots(38)$$

The second transformation manner is that by rotating θ_M and $-\phi_M$ anti-clockwise around O_LZ_L and O_LY_L in turn, the re-entry coordinate system can be transformed to the velocity azimuth co-ordinate system directly. The rotational angular velocity of the velocity azimuth coordinate system with respect to re-entry coordinate system can be described as

$$\overline{\Omega} = -\dot{\phi}_M + \dot{\theta}_M \quad \cdots(39)$$

Similarly, components of the vector $\overline{\Omega}$ with respect to velocity azimuth coordinate system can be derived as

$$\begin{bmatrix}\overline{\Omega}_{x_A}\\ \overline{\Omega}_{y_A}\\ \overline{\Omega}_{z_A}\end{bmatrix} = \begin{bmatrix}0\\ -\dot{\phi}_M\\ 0\end{bmatrix} + L_y(-\phi_M)\begin{bmatrix}0\\ 0\\ \dot{\theta}_M\end{bmatrix} = \begin{bmatrix}\dot{\theta}_M\sin\phi_M\\ -\dot{\phi}_M\\ \dot{\theta}_M\cos\phi_M\end{bmatrix} \quad \cdots(40)$$

From (38) and (40), we can get that

$$\begin{cases}-\dot{\phi}_M = \cos\Delta_\gamma[-\dot{\theta}\sin\Delta_\phi\sin(\Delta_\theta-\phi)+(\dot{\Delta}_\theta-\dot{\phi})\cos\Delta_\phi]\\ \qquad +\sin\Delta_\gamma[\dot{\theta}\cos(\Delta_\theta-\phi)-\dot{\Delta}_\phi]\\ \dot{\theta}_M\cos\phi_M = -\sin\Delta_\gamma[-\dot{\theta}\sin\Delta_\phi\sin(\Delta_\theta-\phi)+(\dot{\Delta}_\theta-\dot{\phi})\cos\Delta_\phi]\\ \qquad +\cos\Delta_\gamma[\dot{\theta}\cos(\Delta_\theta-\phi)-\dot{\Delta}_\phi]\end{cases} \quad \cdots(41)$$

Furthermore, according to the relation equations of Euler angles, we have

$$L_x(\Delta_\gamma) = L_y(-\phi_M)L_z(\theta_M-\theta)L_y(\phi-\Delta_\theta)L_z(\Delta_\phi) \quad \cdots(42)$$

Then, we get

$$\begin{aligned}\sin\Delta_\gamma &= \sin(\Delta_\theta-\phi)\sin(\theta-\theta_M)\\ \cos\Delta_\gamma &= -\sin(\Delta_\theta-\phi)\cos(\theta-\theta_M)\sin\phi_M+\cos(\Delta_\theta-\phi)\cos\phi_M\end{aligned} \quad \cdots(43)$$

Suppose that the gravity acceleration of the vehicle is parallel with O_LZ_L of the re-entry co-ordinate system and points to the earth centre, then the dynamic equations of the vehicle with respect to the velocity azimuth coordinate system can be described as[24]

$$\begin{cases}\frac{\dot{V}_M}{g} = n_{X_A}-\sin\phi_M\\ \frac{V_M}{g}\dot{\theta}_M\cos\phi_M = n_{Y_A}\\ \frac{V_M}{g}\dot{\phi}_M = n_{Z_A}-\cos\phi_M\end{cases} \quad \cdots(44)$$

where n_{X_A}, n_{Y_A} and n_{Z_A} are the components of overload of the vehicle with respect to velocity azimuth coordinate system.

From (41) and (44), the guidance law in the form of normal overload can be given by

$$\begin{cases} n_{Y_A} = \frac{V_M}{g}\{-\sin\Delta_\gamma[-\dot{\theta}\sin\Delta_\phi\sin(\Delta_\theta-\phi)+(\dot{\Delta}_\theta-\dot{\phi})\cos\Delta_\phi] \\ \quad +\cos\Delta_\gamma[\dot{\theta}\cos(\Delta_\theta-\phi)-\dot{\Delta}_\phi]\} \\ n_{Z_A} = -\frac{V_M}{g}\{\cos\Delta_\gamma[-\dot{\theta}\sin\Delta_\phi\sin(\Delta_\theta-\phi)+(\dot{\Delta}_\theta-\dot{\phi})\cos\Delta_\phi] \\ \quad +\sin\Delta_\gamma[\dot{\theta}\cos(\Delta_\theta-\phi)-\dot{\Delta}_\phi]\}+\cos\phi_M \end{cases} \quad \cdots(45)$$

where $\dot{\Delta}_\theta$ and $\dot{\Delta}_\phi$ are respectively given by (24) and (35). $\sin\Delta_\gamma$ and $\cos\Delta_\gamma$ are given by (43). Δ_θ, Δ_ϕ can be obtained as

$$\begin{cases} \Delta_\theta = \begin{cases} -\arcsin\left(v_{e_\phi} \Big/ \sqrt{v_{e_r}^2+v_{e_\phi}^2}\right), v_{e_r} \geq 0 \\ \pi+\arcsin\left(v_{e_\phi} \Big/ \sqrt{v_{e_r}^2+v_{e_\phi}^2}\right), v_{e_r} < 0 \end{cases} \\ \Delta_\phi = \begin{cases} -\arcsin\left(v_{e_\theta} \Big/ \sqrt{v_{e_r}^2+v_{e_\theta}^2+v_{e_\phi}^2}\right), v_{e_r} \geq 0 \\ \pi+\arcsin\left(v_{e_\theta} \Big/ \sqrt{v_{e_r}^2+v_{e_\theta}^2+v_{e_\phi}^2}\right), v_{e_r} < 0 \end{cases} \end{cases} \quad \cdots(46)$$

where v_{e_r}, v_{e_θ} and v_{e_ϕ} are the components of the velocity vector $\mathbf{V_M}$ with respect to LOS coordinate system.

4.0 SIMULATION AND ANALYSIS

4.1 Simulation conditions

Simulation conditions are presented in Table 1. In addition, the vehicle-borne engine is turned off when terminal guidance begins and the simulation stops when the vehicle reaches the ground.

Table 1
Simulation conditions for vehicle and target

Simulation parameters	Specific values
Vehicle initial position (m)	[0, 0, 30,000]
Vehicle initial velocity (m/s)	[1,598, 581, 0]
Vehicle mass (kg)	500
Vehicle reference area (m^2)	1
Available normal overload	5
Target initial position (m)	[100,000, 0, 0]
Target velocity (m/s)	[0, 0, 0]
Guidance parameters	$r_f = 0.001$, $\phi_f = -60°$
Guidance step (s)	0.015

4.2 Simulation results

Under the conditions above, the terminal miss distance is 0.0025 m and the terminal elevation angle of LOS is $-60°$. Terminal velocity of the vehicle is 819.5597 m/s and the full time of flight is 76.4876 s.

The ranges of heading angle, flight path angle, azimuth angle and elevation angle with respect to LOS range are presented in Fig. 2. The ranges of LOS angular rates with respect to LOS range are presented in Fig. 3. We can see that the initial deviation between the heading angle and azimuth angle is 20°, and with LOS range decreasing, the deviation gradually reduces to zero, by which the azimuth angular rate of LOS is confined to zero. The initial deviation between the flight path angle and elevation angle is 16.7°. With LOS range

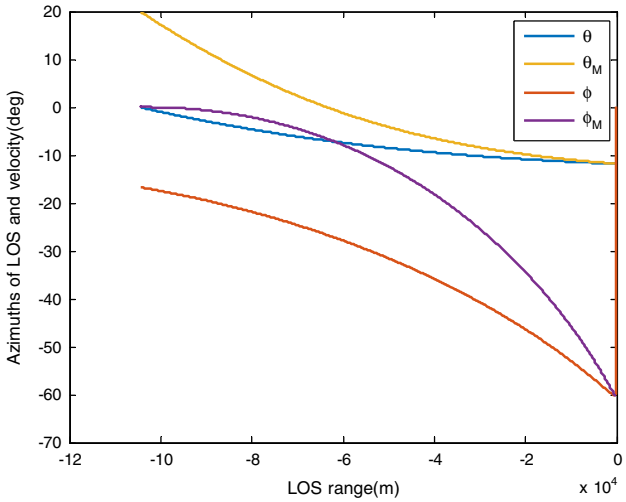

Figure 2. Azimuths of LOS and velocity.

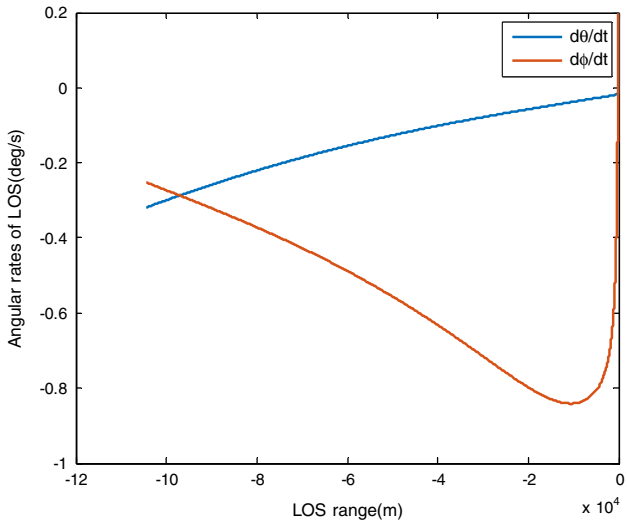

Figure 3. Angular rates of LOS.

decreasing, the deviation first becomes larger to guarantee the impact angle constraint, and then gradually tends to be zero, which guarantees the elevation angular rate of LOS converges to zero. Both the terminal flight path angle and elevation angle are −60°, demonstrating that the impact angle constraint is satisfied.

Response of normal overloads for guidance command with respect to LOS range are presented in Fig. 4, from which we can see that initial normal overload of the yaw motion is relatively large and it gradually reduces with the decreasing of azimuth angular rate of LOS. Normal overload of the pitch motion varies from the positive value to the negative value, by which the flight path angle increases firstly and then decreases to satisfy the impact angle constraint. What is more, the normal overloads for guidance command vary smoothly during the whole flight, which is convenient for the implementation of attitude control system.

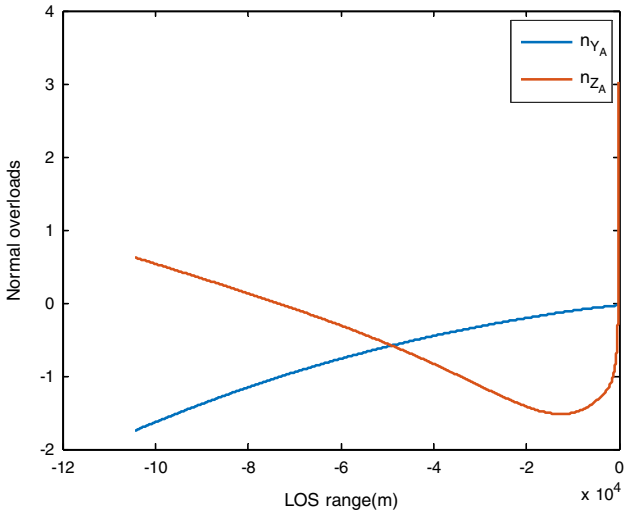

Figure 4. Normal overloads for guidance command.

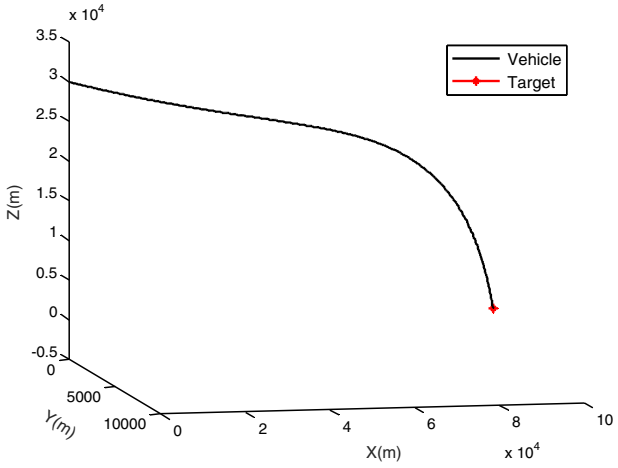

Figure 5. 3D re-entry trajectory.

Profile of 3D re-entry trajectory is presented in Fig. 5, from which we can see that with the LOS angular rates converging to zero, the vehicle flies close to the target and ultimately attacks the target with desired impact angle and satisfactory precision. The results shown in simulation are consistent with the theory that the guidance law is based on, demonstrating the correctness and validity of the novel guidance model and guidance law.

5.0 CONCLUSION

Aiming at 3D terminal guidance problem, a novel guidance model with respect to LOS range is established, based on which optimal re-entry guidance law with impact angle constraint is designed. Contributions of this paper are mainly twofold:

(1) A novel guidance model is established, in which LOS range is treated as independent variable to describe the relative motion between the vehicle and the target. The guidance model includes two differential equations that describe LOS's pitch and yaw motions in which the pitch motion is separately decoupled. This model avoids the inaccuracy of simplified 2D guidance model and the complexity of 3D coupled guidance model, which not only maintains the accuracy but also simplifies the guidance law design.

(2) Application of the novel guidance model is studied for optimal re-entry guidance problem with impact angle constraint. By transformation of the guidance model, the guidance law design problem is transformed to the linear quadratic optimal control problem. Then optimal re-entry guidance law of the pitch and yaw motion of LOS are designed, respectively, theoretically proving that angular rate of LOS converges to zero and elevation angle converges to the desired impact angle. Compared with the optimal guidance laws based on traditional guidance model, the proposed one based on novel guidance model is implemented with the LOS range instead of time-to-go, which avoids the problem of the time-to-go estimation of traditional optimal guidance laws. Simulation results show the correctness and validity of the novel guidance model and guidance law.

REFERENCES

1. CHEN, K.J. and ZHAO, H.Y. An optimal reentry maneuver guidance law applying to attack the ground fixed target, *J of Astronautics*, 1994, **15**, (1), pp 1–7.
2. ZHAO, H.Y. Dynamics and Guidance of Reentry Vehicle, 1997.
3. MOON, J., KIM, K. and KIM, Y. Design of Missile Guidance Law via Variable Structure Control, *J of Guidance, Control and Dynamics*, 2001, **24**, (4), pp 659–664.
4. YAMASAKI, T., BALAKRISHNAN, S.N., TAKANO, H. and YAMAGUCHI, I. Sliding mode-based intercept guidance with uncertainty and disturbance compensation, *J of the Franklin Institute-Engineering and Applied Mathematics*, 2015, **352**, (11), pp 5145–5172.
5. GENG, F. and ZHU, X.P. The Research of nonlinear robust guidance law for high speed unmanned attack air vehicle, *J of Astronautics*, 2008, **29**, (5), pp 922–927.
6. LECHEVIN, N. and RABBATH, C.A. Lyapunov-based nonlinear missile guidance, *J of Guidance, Control and Dynamics*, 2004, **27**, (5), pp 1096–1102.
7. WANG, X.H. and WANG, J.Z. Partial integrated missile guidance and control with finite time convergence, *J of Guidance, Control and Dynamics*, 2013, **36**, (5), pp 1399–1409.
8. LI, G.L., YAN, H. and JI, H.B. A guidance law with finite time convergence considering autopilot dynamics and uncertainties, *Int J of Control Automation and Systems*, 2014, **12**, (5), pp 1011–1017.

9. QU, P.P., SHAO, C.T. and ZHOU, D. Finite time convergence guidance law accounting for missile autopilot, *J of Dynamic Systems Measurement and Control*, 2015, **137**, (5), pp 1–8.
10. SONG, S.H. and HA, I.J. A Lyapunov-like approach to performance analysis of 3-dimensional pure PNG laws, *IEEE Transactions on Aerospace and Electronic Systems*, 1994, **30**, (1), pp 238–247.
11. OH, J.H. and HA, I.J. Capturability of the 3-dimensional pure PNG law, *IEEE Transactions on Aerospace and Electronic Systems*, 1999, **35**, (2), pp 491–503.
12. YANG, C.D. and YANG, C.C. Analytical solution of three-dimensional realistic true proportional navigation, *J of Guidance, Control and Dynamics*, 1996, **19**, (2), pp 569–577.
13. YANG, C.D. and YANG, C.C. Analytical solution of 3D true proportional navigation, *IEEE Transactions on Aerospace and Electronic Systems*, 1996, **32**, (3), pp 1509–1522.
14. WU, L.J. Designing method of robust dynamic inversion for 3-D terminal guidance law, *Systems Engineering and Electronics*, 2007, **29**, (8), pp 1331–1333.
15. ZHU, J.W., LIU, L.H., TANG, G.J. and BAO, W.M. Three-dimensional nonlinear coupling guidance for hypersonic vehicle in dive phase, *Science China Technological Sciences*, 2014, **57**, (9), pp 1824–1833.
16. WEISS, G. and RUSNAK, I. All-aspect three-dimensional guidance law based on feedback linearization, *J of Guidance, Control and Dynamics*, 2015, **38**, (12), pp 2421–2428.
17. CHEN, B.S., CHEN, Y.Y. and LIN, C.L. Nonlinear fuzzy H_∞ guidance law with saturation of actuators against maneuvering targets, *IEEE Transactions on Control Systems and Technology*, 2002, **10**, (6), pp 769–779.
18. SHIEH, C.S. Design of three-dimensional missile guidance law via tunable nonlinear H-infinity control with saturation constraint, *IET Control Theory and Applications*, 2007, **1**, (3), pp 756–763.
19. MOOSAPOUR, S.S., ALIZADEH, G., KHANMOHAMMADI, S. and MOOSAPOUR, S.H. A novel nonlinear robust guidance law design based on SDRE technique, *Int J of Aeronautical and Space Sciences*, 2012, **13**, (3), pp 369–376.
20. GUO, C. and LIANG, X.G. Guidance law for near space interceptor based on block backstepping sliding mode and extended sate observer, *Int J of Aeronautical and Space Sciences*, 2014, **15**, (2), pp 163–172.
21. YUAN, Y.B. and ZHANG, K. Design of a robust guidance law via active disturbance rejection control, *J of Systems Engineering and Electronics*, 2015, **26**, (2), pp 353–358.
22. ZHANG, Z.X., MAN, C.Y., LI, S.H. and JIN, S. Finite-time guidance laws for three-dimensional missile-target interception, *Proceedings of the Institution of Mechanical Engineers Part G – J of Aerospace Engineering*, 2016, **230**, (2), pp 392–403.
23. SHAFIEI, M.H. and BINAZADEH, T. Partial stabilization-based guidance, *ISA Transactions*, 2012, **51**, (1), pp 141–145.
24. QIAN, X.F., LIN, R.X. and ZHAO, Y.N. Flight Dynamics of Missile, Beijing Institute of Technology Press, Beijing, 2008.